



Nonlinear Optical Characteristics of Magnesium - Zinc Nano composites

KEYWORDS

Magnesium – Zinc ferrite; Sol Gel technique; Nonlinear Optics.

Rintu Mary Sebastian

Research Department of Physics, Maharaja's College, Enakulam, Kerala, India

Mathew S

International School of Photonics, Cochin University of Science and Technology, Cochin, Kerala, India.

P Radhakrishnan

International School of Photonics, Cochin University of Science and Technology, Cochin, Kerala, India.

E M Mohammed

Research Department of Physics, Maharaja's College, Enakulam, Kerala, India

ABSTRACT

In this paper we report the nonlinear optical properties of Mg – Zn nano crystalline mixed ferrites Prepared by sol-gel technique. The XRD patterns revealed the absence of any impurity peak and points to the formation of pure cubic spinel structure in all the compounds. XRF analysis confirmed the purity of the samples. Saturation magnetization and remanence decreased with zinc doping. The optical limiting properties are investigated using the open aperture z – scan technique. The optical nonlinearity increased and the material shows better optical limiting characteristics at higher zinc doping concentrations. The values of optical limiting parameters of Mg - Zn nano composite makes it a potential material for the development of nonlinear optical devices with a relatively small limiting threshold. To the best of our knowledge a systematic variation of the optical limiting property with doping Concentration has not been reported elsewhere.

Introduction

In the recent past, rapid technological advancement in laser optics demands optical limiting devices to protect eyes and sensor from laser induced radiation damage. An ideal optical limiter should be transparent to low energy laser pulses and opaque at high energy laser radiations. Recently, magnetic nano materials have attracted substantial attention as optical limiter, as the optical properties of such optoelectronic devices are controllable by an external stimulus such as magnetic field [1].

Ferrites are one of the most widely used magnetic oxides with unusual optical, electrical and magnetic properties with respect to their bulk. Of the various ferrites Mg – Zn ferrite is a soft magnetic material with wide range of applications in transformer, deflection antenna, multiple path communication, magnetic liquid, absorbing material etc. Optical nonlinearities in ferrites are relatively unexplored compared to organo - metallic compounds, semiconductors and most recently nanoparticles of metals and semiconductors [2, 3]. Very few studies been reported regarding the optical limiting properties of ferrites. JJ Thomas et al. have reported the optical limiting properties of different nano ferrites with z-scan technique [4]. Optical limiting properties of mixed zinc ferrite have been reported by P. Chanthanasupawaong et al. [5].

However a systematic investigation of optical limiting properties of spinel ferrites with doping concentration has not been thoroughly studied yet. In this paper, we report the variation of optical limiting properties of zinc doped magnesium ferrite, upon illumination of nano second laser pulses at 532 nm.

Experimental Details

$Mg_{1-x}Zn_xFe_2O_4$ ($x = 0.00, 0.25, 0.50, 0.75, 1.00$) were prepared by sol gel technique. Stoichiometric ratio of AR grade Ferric nitrate ($Fe(NO_3)_3 \cdot 9H_2O$), Zinc Nitrate ($Zn(NO_3)_2 \cdot 6H_2O$) and Magnesium Nitrate ($Mg(NO_3)_2 \cdot 6H_2O$), (99.9% pure Merck) were dissolved in ethylene glycol. The solution was heated at 60°C to form a wet gel. The gel was then dried at 120°C for 6hrs, which self-ignites to form a voluminous

of fluffy product. The finely grounded powder was heated at 400°C for 2hrs. The sample suspensions were prepared by dispersing the known quantity of the sample in pure ethylene glycol so as to have a concentration 1.5×10^{-4} mol/L.

The structural characterization of the prepared samples were carried out using BRUKER make AXS D8 ADVANCE powder X – ray Diffractometer with Cu – K α radiation ($\lambda = 1.5406\text{\AA}$) at 40kV and 35mA from 20° to 80° in steps of 0.002° per second. Wavelength dispersive X – ray Florescence spectrometer (WD – XRF) Make: Bruker, Model: S4 PIONEER was used to study the purity of the prepared samples. Magnetic studies at room temperature were carried out using vibrating sample magnetometer (VSM Lakeshore 7410) up to a maximum field of 15kOe. The UV absorption spectra were recorded using UV – Vis Spectrophotometer (Varian, Cary 5000) at room temperature.

Nonlinear optical characterization was done using single beam z – scan technique with nanosecond laser pulse. z-scan technique developed by Sheik Bahae et. al [6, 7] was used to measure the optical nonlinearity and has a sensitivity comparable to interferometry methods. A Q switched neodymium doped yttrium aluminum garnet laser (Spectra Physics LAB – 1760, 532nm, 7ns, 10Hz) was used as the light source. The sample was taken in a 1mm cuvette and was translated in the direction of the incident light near the focal spot of the lens with a focal length of 200mm. The radius of the beam waist ω_0 was calculated to be 43.3 μ m. The Rayleigh length calculated using the equation $z_0 = \frac{\pi \omega_0^2}{\lambda}$ was estimated to be 11mm, which is much greater than the thickness of the sample cuvette (1mm), an essential requirement for z - scan technique. The transmitted beam energy, reference beam energy and their ratio were simultaneously measured by an energy ratio meter (Rj 7620, Laser Probe Corp.), with two identical piezoelectric detector heads (RjP 735). The z scan system is calibrated using CS₂ as the standard. The laser pulse energy used for the experiment was 100 μ J. The effect of fluctuations of laser power is eliminated by dividing the transmitted power by the power obtained at the reference detector. The po-

sition – transmission curve, the open aperture z scan curve thus obtained was analyzed using the procedure described by Bahae et. al [6], and nonlinear absorption coefficients of the sample was obtained by fitting the experimental z scan plot with the theoretical plot.

Results and Discussion

X - Ray Diffraction Studies

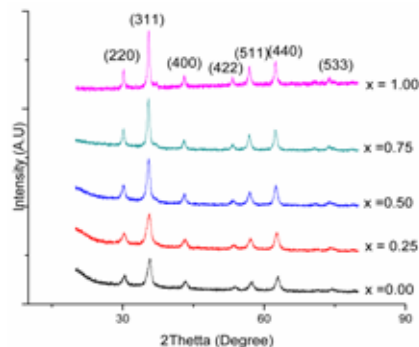


Figure 1: X – ray diffraction pattern of the sample $Mg_{1-x}Zn_xFe_2O_4$.

The X ray diffraction patterns of the samples are shown in figure1. The patterns were compared with the standard file (JCPDS PDF # 03 – 875) and the absence of any impurity phase was confirmed. The crystallite size of all the samples were calculated from the line broadening of the intense peak (311) plane using Scherrer formula [8] and were found to vary from 8 to 18nm. It is found that the crystallite size increased with increase in Zn^{2+} ion concentration. From the XRD patterns it can be noticed that there is a shift of the most intense peak (311) toward lower angles with increase in Zn^{2+} ion concentration, indicating an increase in lattice constant with increase in zinc ion concentration. This could be attributed due to the variation of ionic size difference between Mg^{2+} (0.06nm) and Zn^{2+} ion (0.074nm).

XRF Analysis

The quantitative compositional analysis of the prepared samples was done using WD – XRF measurements. The results of the measurements are tabulated in Table 1.

Table 1: XRF analysis of $Mg_{1-x}Zn_xFe_2O_4$ with $x = 0.00$ and $x = 0.05$.

	$ZnFe_2O_4$		$Zn_{0.5}Mg_{0.5}Fe_2O_4$	
Elements present	Concentration in $ZnFe_2O_4$ (%)	Expected Concentration in $ZnFe_2O_4$ (%)	Concentration in $Zn_{0.5}Mg_{0.5}Fe_2O_4$ (%)	Expected Concentration in $Zn_{0.5}Mg_{0.5}Fe_2O_4$ (%)
Fe	45.370	46.331	49.570	50.646
O	26.500	26.548	5.677	5.511
Zn	26.170	27.121	29.100	29.100
Mg	Nil	Nil	14.010	14.823

From the values in table 1 it is clear that the obtained values are in good agreement with the theoretical values.

Magnetic Measurements

Magnetic characterization of the samples was carried out using a vibration sample magnetometer at room temperature for a maximum applied field of 15kOe. It is found that the M – H curves doesn't saturate even at an applied magnetic field of 15kOe, which could be due to the high magneto crystalline anisotropy associated with ferrites [9].

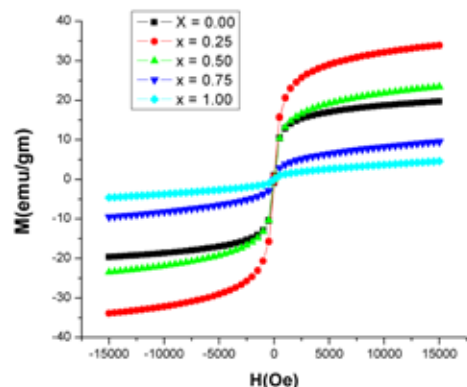


Figure 2: Hysteresis curve of $Mg_{1-x}Zn_xFe_2O_4$ samples

The M_s values of all the samples were calculated by extrapolating the inverse of the field versus magnetization (M_s) graph to $1/H_c = 0$ [10]. The saturation magnetization (M_s), remanence (M_r) and remanent ratio ($R = M_r/M_s$) for the various samples are shown in table 2.

Table 2: Effect of Zn^{2+} ion substitution on magnetic parameters of $MgFe_2O_4$

x	Particle Size (nm)	M_s (emu/g)	M_r (emu/g)	$R = M_r/M_s$ (10^{-2})
0.00	9.70±0.20	20.22	0.984	1.10
0.25	8.57±0.29	34.51	0.768	0.38
0.50	11.73±0.22	23.99	0.187	0.78
0.75	15.27±0.29	9.77	0.037	2.23
1.00	18.65±0.32	5.25	0.058	4.87

The saturation magnetization was found to decrease with increase in Zn^{2+} ion concentration, whereas pure magnesium ferrite showed a lower value of saturation magnetization compared to $Mg_{0.75}Zn_{0.25}Fe_2O_4$. The reduction in M_s could be related to the variation of cationic distribution in the spinel structure as chemical composition is modified. Similar behavior was reported with Zinc doping by Hajar-pour et. al. [11].

The remanence value was found to decrease with increase in Zn^{2+} ion concentration. The low value of remanence implies that domains can move easily in response to the magnetic fields indicating increase in isotropic property with increase in Zinc ion concentration. This indicates the possibility of tuning the magnetic parameters in $MgFe_2O_4$ with Zn^{2+} ion doping.

Optical Studies

The optical absorption spectra of the samples were recorded using the UV - Vis spectrophotometer (Varian, Cary 5000). As usual the absorption spectra didn't show any definite absorption peaks. The band gap E_g for each sample was determined from the equation [12].

$$ah\nu = A(h\nu - E_g)^n \quad \text{----- (1)}$$

where $h\nu$ is the photon energy, A is a constant α linear absorption coefficient. The value of n depends on the type of transition; $n = 1/2$ for direct allowed transition, $n = 3/2$ for direct forbidden transition, $n = 2$ for indirect allowed transition, $n = 3$ for indirect forbidden transition. For all the samples the best fit was obtained for $n = 1/2$. [4].

Thus the E_g values are determined by extrapolating the linear portion of the Tauc plots, the graph between $(ah\nu)^2$ versus $h\nu$ plot, to the point $\alpha = 0$. The variation of band gap with Zn^{2+} ion concentration is given in Table 3. The optical band gap (E_g) is found to depend on composition and crystal structure. It is seen that band gap decreases with increase in Zn^{2+} ion concentration, but an unexpected low value was found for pure magnesium ferrite compared to $Mg_{0.75}Zn_{0.25}Fe_2O_4$, which could be related to variation of cationic distribution in spinel ferrite.

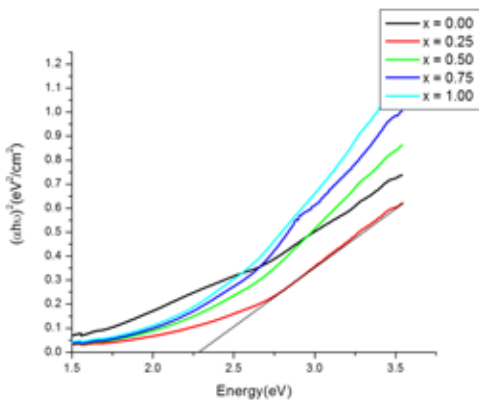


Figure 3: Tauc plots of Mg – Zn ferrite series for calculating the band gap energies.

Table 3: Sample composition, Average particle size, band gap of Mg – Zn ferrite series.

Samples	Particle Size (nm)	Band Gap (ev)
$MgFe_2O_4$	9.70 ± 0.20	1.884
$Mg_{0.75}Zn_{0.25}Fe_2O_4$	8.57 ± 0.29	2.271
$Mg_{0.5}Zn_{0.5}Fe_2O_4$	11.73 ± 0.22	2.226
$Mg_{0.25}Zn_{0.75}Fe_2O_4$	15.27 ± 0.29	2.203
$ZnFe_2O_4$	18.65 ± 0.32	2.175

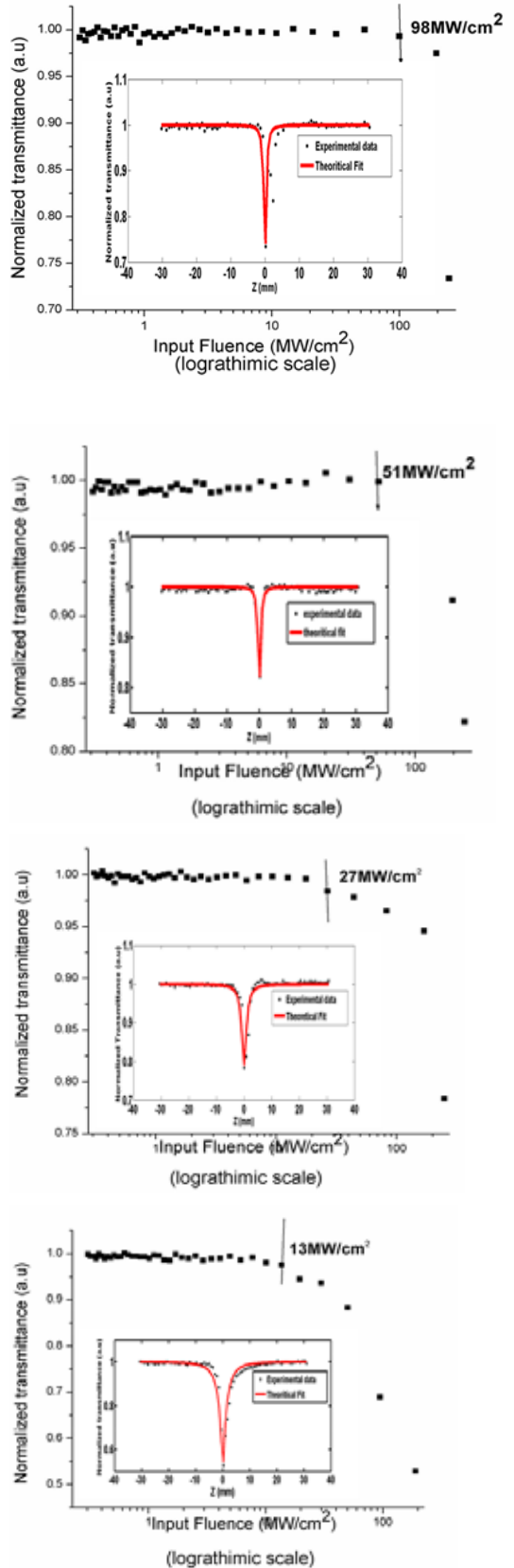


Figure 4: Optical limiting curves for Mg – Zn series (a) $MgFe_2O_4$ (b) $Mg_{0.75}Zn_{0.25}Fe_2O_4$ (c) $Mg_{0.5}Zn_{0.5}Fe_2O_4$ (d) $ZnFe_2O_4$ for input pulse energy of $100 \mu J$. Inset shows the corresponding open aperture z-scan curves. Solid lines repre-

sent the numerical fits and circular points the measured data points.

Figure (4) depicts the optical limiting curves of the typical samples with Zn²⁺ concentration x = 0.00, 0.25, 0.75, 1.00. The z-scan data point obtained for all the samples were numerically fitted to the transmission equation for (TPA) process.

$$T(z) = \frac{c}{q_0\sqrt{\pi}} \int_{-\infty}^{\infty} L_n(1 + q_0 e^{-t^2}) dt \dots\dots\dots (2)$$

$$\text{Where } q_0(z, r, t) = \beta I_0(t) L_{eff} \dots\dots\dots (3)$$

L_{eff} is the effective thickness with linear absorption coefficient α and β is the nonlinear absorption coefficient. I₀ is the irradiance at the focus.

$$L_{eff} = 1 - e^{-\alpha l} \dots\dots\dots (4)$$

The solid curves in Fig (4) are the theoretical fit and the circular points represent the experimental data. Normalized transmittance valley in the z-scan plots indicates the occurrence of an enhanced absorption process like Reverse Saturable Absorption (RSA) [13]. The obtained values of the nonlinear absorption coefficient β at an intensity of 100μJ are shown in table 4.

Table 4: Table showing the input pulse energy and nonlinear absorption coefficients for different doping concentrations.

Samples	Input Laser Energy (μJ)	β (m/W)
MgFe ₂ O ₄	100	4.77 × 10 ⁻¹⁰
Mg _{0.75} Zn _{0.25} Fe ₂ O ₄	100	2.74 × 10 ⁻¹⁰
Mg _{0.5} Zn _{0.5} Fe ₂ O ₄	100	2.89 × 10 ⁻¹⁰
Mg _{0.25} Zn _{0.75} Fe ₂ O ₄	100	3.23 × 10 ⁻¹⁰
ZnFe ₂ O ₄	100	5.52 × 10 ⁻¹⁰
	85	3.76 × 10 ⁻¹⁰
	65	2.53 × 10 ⁻¹⁰

The significant optical nonlinearities of CdS nano crystals was reported to be of the order of 10⁻¹⁰ m/W [14], whereas for Ag₂S – CdS nano composites, organic coated quantum dots, metal clusters etc, yielded values of the order of 10⁻⁹ to 10⁻¹⁴ m/W [15, 16], Polydiacetylene nanocomposites reported β values of the order 10⁻¹¹m/W[17]. From the obtained values of β and previously reported values it is evident that spinel ferrites are potential candidates for optical limiting applications. From the tabular column (4) it's clear that the nonlinear absorption coefficient increases with Zn²⁺ ion concentration, whereas shows a high value of nonlinear absorption coefficient for pure MgFe₂O₄. The general cationic distribution can be represented as M_δ²⁺Fe_{1-δ}²⁺[M_{1-δ}²⁺Fe_δ²⁺]₄O₄, where the cations inside the bracket are located in octahedral sites and the other outside the bracket in tetrahedral sites. For δ = 1, it's called normal spinel, for δ = 0 it's called inverse spinel and if δ is between 0 and 1 it is mixed spinel structure. ZnFe₂O₄ has normal spinel structure with all the Zn²⁺ ions distributed in the tetrahedral sites and ferric ions occupy the octahedral sites. In a mixed spinel structure with δ between 0 to 1, both the tetrahedral and octahedral sublattices sites are

occupied by divalent and trivalent ions. Neutron diffraction examinations of MgFe₂O₄ have yielded a value of δ approximately equal to 0.1 [18]. Magnesium ferrite is a typical spinel in which the cationic distribution in the crystal lattice site is very sensitive to heat treatments, due to the high diffusibility of Mg²⁺ ions [19, 20]. Zn doped MgFe₂O₄ are mixed ferrites which show the combination of these two structural orientations. The amount of Fe³⁺ ions in the octahedral sites determines the polarization in ferrites [21]. Hence polarization depends on the spinel structure.

ZnFe₂O₄ has maximum number of Fe³⁺ ions in the octahedral site and hence highest polarization and eventually contribute to the nonlinear absorption. Similar effect has been reported by J. J Thomas et. al. [4].

The observed intensity dependent nonlinear absorption can be due to various mechanisms like two photon absorption (2PA), free carrier absorption (FCA), excited state absorption (ESA), nonlinear scattering etc. In the present case, the excitation photon energy is 2.3eV from the calculated values of band gap tabulated in table (3), the excitation wavelength (532nm) does not fulfill the 2PA requirement (hν > E_g/2). Hence the role of 2PA in the observed nonlinear absorption behavior is less prominent and therefore can be neglected. According to literature, absorption coefficient β decreases with increase in input laser pulse energy for ESA [22]. But here when z- scan measurements were performed for three different pulse energies (65μJ, 85μJ, 100μJ), it was found that β value increased substantially with increase in input pulse energy there by ruling out ESA contribution. Hence the occurrence of higher order nonlinear processes such as free carrier absorption is the mechanism suggested for NLA.

To examine the viability of Zn – Mg mixed nano ferrites as optical limiters; the nonlinear transmission of the colloids is studied as a function of input fluence. The fluence value for all the positions can be calculated using the standard equation for Gaussian beam waist and fluence at the focus. Such plots generated from the z-scan trace provide a better comparison of the nonlinear absorption or transmission of the samples. The arrow in the figures indicates the approximate fluence at which normalized transmission begins to deviate from linearity.

Limiting threshold is an important parameter in optical limiting measurements. Lower the optical limiting threshold; better will be the optical limiting response [23]. From the β values in the table (4) and figure (4) it's clear that with increase in zinc doping the nonlinear absorption coefficient (β) increases and the optical limiting threshold decrease. It can be concluded that the material shows better optical limiting characteristics at higher zinc doping concentrations.

Conclusions

Mg_{1-x}Zn_xFe₂O₄ with x = 0.00, 0.25, 0.50, 0.75, 1.00 were prepared using sol gel technique and their optical limiting property were investigated using nano second laser pulses at 532nm. The XRD patterns revealed pure cubic spinel structure without any impurity phase in all the samples. XRF analysis confirmed the purity of the prepared samples. Saturation magnetization and remanence decreased with zinc doping. The z-scan studies showed that optical nonlinearity increased with zinc ion doping with increase in polarization effect. The obtained optical limiting parameters show that these materials are efficient optical limiters and the limiting thresholds are lower at higher zinc con-

centrations. A major advantage of ferro fluids is that optical properties in these materials are tunable by the applied magnetic field, pointing to magneto controllability in device applications.

REFERENCE

- [1]. J. Chen, X. Chen, S. Pu, Z. Di and Y. Xia (2007) Realization of optical limiting with a magnetic fluid film. *Opt. Commun.*, 276, 268 – 271. <http://doi:10.1016/j.optcom.2007.04.030>. [2]. RA. Ganeev, Al. Rysanyansky, Sh. R. Kamalov, MK. Kadrov and T. Usmanov (2001) Nonlinear susceptibilities, absorption coefficients and refractive indices of colloidal metal, *J. Phys D: Appl. Phys.*, 34, 1602 – 1611. <http://doi:10.1088/0022-3727/34/11/308>. [3]. GX. Chen, MH. Hong, TC. Chong, HI. Elim, GH. Ma and W. Ji (2004) Preparation of carbon nanoparticles with strong optical limiting properties by laser ablation in water, *J. Phys D: Appl. Phys.*, 95, 1455 – 1459. <http://dx.doi.org/10.1063/1.1637933>. [4]. JJ. Thomas, S. Krishnan, K. Sridharan, R. Philip and N. Kalarikkal (2012) A comparative study on the optical limiting properties of different nano ferrites with Z scan technique, *Material Research Bulletin*, 47, 1855 - 1860. <http://dx.doi.org/10.1016/j.materresbull.2012.04.067>. [5]. P. Chantharasupawong, R. Philip, T. Endo and J. Thomas (2012) Enhanced optical limiting in Nanosized mixed zinc ferrites, *Appl. Phys. Lett.*, 100, 221108 (4pp). <http://dx.doi.org/10.1063/1.4724194>. [6]. Mnsoor Sheik Bahae, Ali A. Said, Tai Huei Wei, David J. Hagan and E.W. Van Stryland (1990) Sensitive measurements of optical nonlinearities using a single beam, *IEEE Journal of quantum Electronics*, vol. 26 4. <http://www.optics.unm.edu/sbahae/publications/z-scan-IEEE-JQE90.pdf>. [7]. Litty Irimpan, B. Krishnan, V.P.N. Nampoori and P. Radhakrishnan, Luminescence tuning and enhanced nonlinear optical properties of nanocomposites of ZnO – TiO₂ (2008) *J. Appl. Phys.* 103, 094914. <http://doi:10.1117/1.3589297>. [8]. Rintu Mary Sebastian, Smitha Thankachan, Sheena Xavier, Shaji Joseph, and E. M. Mohammed (2014) Structural and magnetic properties of chromium doped zinc ferrite, *AIP Conference Proceedings* 1576, 91. <http://doi:10.1063/1.4861990>. [9]. BG. Taksha, SE. Shirsath, SM. Pantage and KM. Jadhav (2008) Structural investigations and magnetic properties of cobalt ferrite nanoparticles prepared by sol – gel auto combustion method solid state communications, 147 479 – 483. <http://doi:10.1016/j.ssc.2008.06.040>. [10]. A. Kale, S. Gubbala, RDK. Misra (2004) Magnetic behavior of Nanocrystalline nickel ferrite synthesized by reverse micelle technique *Journal of Magnetism and Magnetic Materials*, 277, 350 – 358. <http://doi:10.1016/j.jmmm.2003.11.015>. [11]. S. Hajarpour, A. Honorbakhsh Raoui, Kh. Gheisari (2014) Structural evolution and magnetic properties of Nanocrystalline magnesium – zinc soft ferrites synthesized by glycine – nitrate combustion process, *Journal of Magnetism and Magnetic Materials*, 363, 21 – 25. <http://doi:10.1016/j.jmmm.2014.03.027>. [12]. J. Tauc, *Amorphous and Liquid Semiconductors*, 1st ed., Plenum Press, New York, 1974. [13]. P. P. Kiran, D. R. Reddy, B. G. Maiya, and D. N. Rao (2002) Third Order Nonlinearity and Optical Limiting Studies in Phosphorus (V) Porphyrins with Charge Transfer States, *Optical Materials* 21, 565-568. [http://doi:10.1016/S0925-3467\(02\)00201-X](http://doi:10.1016/S0925-3467(02)00201-X). [14]. N. Venkatram, R. Sai Santosh Kumar, and D. Narayana Rao (2006) Nonlinear absorption and scattering properties of cadmium sulphide nanocrystals with its application as a potential optical limiter, *J. Appl. Phys.*, 100, 074309. <http://doi:10.1063/1.2354417>. [15]. M. Y. Han, W. Huang, C. H. Chew, L. M. Gan, X.-J. Zhang and W. Ji (1998) Large nonlinear absorption in coated Ag₂S/CdS nanoparticles by inverse microemulsion, *J. Phys. Chem. B*, 102, 1884-1887. <http://doi:10.1021/jp972877z>. [16]. S. Shi, W. Ji, S. H. Tang, J. P. Lang and X. Q. Xin (1994) Synthesis and Optical Limiting Capability of Cubane-like Mixed Metal Clusters (n-Bu₄N)[3MoAg₃BrX₃S₄] (X = Cl and I), *J. Am. Chem. Soc.*, 116 (8), pp 3615–3616. <http://doi:10.1021/ja00087a064>. [17]. Chen Xin, Zou Gang, Deng Yan and Zhang Qijin. (2008) Synthesis and nonlinear optical properties of nanometer-size silver-coated polydiacetylene composite vesicles [J]. *Nanotechnology* (19), 195703. <http://doi:10.1088/0957-4484/19/19/195703>. [18]. G. E. Bacon and F. F. Roberts (1953) Neutron-diffraction studies of magnesium ferrite-aluminate powders, *Acta Cryst.* 6, 57-62. <http://doi:10.1107/S0365110X53000132>. [19]. E.W. Gorter (1950) Magnetization in ferrites; saturation magnetization of ferrites with spinel structure, *Nature*, 20, 165(4203), 798-800. [20]. V. B. Kawade, G. K. Bichile and K. M. Jadhav (2000) X-ray and infrared studies of chromium substituted magnesium ferrite, *Mater Lett* 42(1-2), pp. 33-37. [http://doi:10.1016/S0167-577X\(99\)00155-X](http://doi:10.1016/S0167-577X(99)00155-X) [21]. K. M. Batoo (2011) Study of dielectric and impedance properties of Mn ferrites, *Physica B* 406, 382 – 387. <http://doi:10.1016/j.physb.2010.10.075>. [22]. G. S. Sree Kumar, P.G. Louie Frobel, S. Sreeja, S.R. Suresh, S. Mayadevi, C.I. Muneera, C.S. S. Sandeep, R. Philip and C. Mukhaejee (2011) Nonlinear absorption and photoluminescence emission in nanocomposite films of Fuchine basic dye – polymer system, *Chemical Physics Letters* 506 61 – 65. <http://doi:10.1023/A:1019708430947>. [23]. Litty Irimpan, V.P.N. Nampoori and P. Radhakrishnan (2008) Spectral and nonlinear optical characteristics of nano composites of ZnO – CdS, *J. Appl. Phys.* 103 094914. <http://doi:10.1063/1.2919109>.